Highly Stable Membranes of Poly(phenylene sulfide benzimidazole) Cross-Linked with Polyhedral Oligomeric Silsesquioxanes for High-Temperature Proton Transport

Viviani, Marco; Fluitman, Sebastiaan Pieter; Loos, Katja; Portale, Giuseppe

Link to publication in University of Groningen/UMCG research database

Highly Stable Membranes of Poly(phenylene sulfide benzimidazole) Cross-Linked with Polyhedral Oligomeric Silsesquioxanes for High-Temperature Proton Transport

Marco Viviani, Sebastiaan Pieter Fluitman, Katja Loos, and Giuseppe Portale*

Cite This: *ACS Appl. Energy Mater.* 2020, 3, 7873–7884

Read Online

ACCESS | Metrics & More | Article Recommendations | Supporting Information

ABSTRACT: Poly(phenylene sulfide benzimidazole) has been synthesized and tested as a potential material for high-temperature proton transport. A high content of sulfide bonds has been implemented in the polymer chains to endow a high antioxidant capacity and, in combination with bulky benzimidazole pendant units, to significantly suppress crystallinity and thereby improve the solubility in highly polar aprotic solvents. The amorphous polymer has high thermal stability and high glass transition temperature (T_g). Freestanding, insoluble, and robust membranes were obtained via thermal cross-linking of the benzimidazole moieties with octaglycidyl polyhedral oligomeric silsesquioxane (g-POSS). The series of hybrid networks (cPPSBi_X, with X being the g-POSS content wt %) showed excellent oxidative stability, with cPPSBi_15 having weight loss lower than 5% after 264 h in Fenton's reagent at 80 °C. Elastic moduli as high as 868 MPa with reduced strain at break (1.8%) were obtained. After doping the membranes with phosphoric acid, proton conductivity in the range of 2.3×10^{-2} S cm^{-1} at 180 °C was obtained, and the membranes show a stress at break of 2.3 MPa. Dimensional and mechanical stability were maintained also at high doping levels thanks to the inclusion of g-POSS which provides the resulting hybrid networks with increased free volume and high cross-link density.

KEYWORDS: high-temperature polymer electrolyte membrane (HT-PEM), anhydrous proton conductivity, oxidative stability, hybrid composites, cross-linked membranes, benzimidazole, POSS
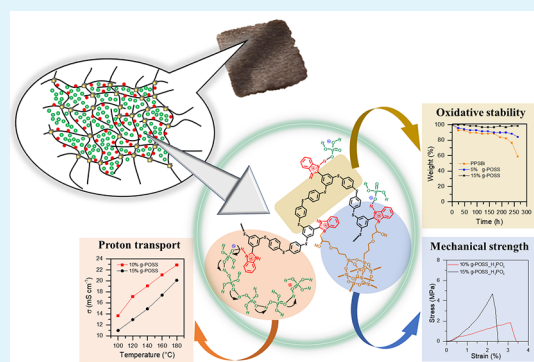
INTRODUCTION

Fuel cells are devices that convert hydrogen and water into electricity, water, and heat. Among the different types and classifications, polymer electrolyte (or proton exchange) membrane fuel cells (PEMFCs) have been intensively studied, and nowadays, they are the most used thanks to their high efficiency, compact design, wide range of applications, low emissions, and environmental friendliness.[1,2] Proton exchange membrane fuel cells could be classified according to their operative temperature in low-temperature PEM fuel cells (LT-PEMFCs) and High-Temperature PEM fuel cells (HT-PEMFCs). LT-PEMFCs work between 20 and 80 °C using PFSA (perfluorosulfonic acids) membranes, such as Nafion, which perform best under fully hydrated conditions, reaching a conductivity as high as 0.1 S cm^{-1} at 30 °C and 80% relative humidity (RH).[3] The high performances of these systems come at the expense of several drawbacks regarding water management inside the membrane electrode assembly (MEA), slow oxidative reduction reaction (ORR) kinetics, high sensitivity to CO poisoning by the Pt catalyst, and high costs of the catalyst and high-purity hydrogen supply.[4−6] HT-PEMFCs offer potential solutions to all of these issues as they work in the range between 100 and 200 °C (preferably 120–

180 °C) where Pt catalyst becomes more tolerant to CO contamination up to 3% above 150 °C,[7,8] the kinetics of the ORR increase and thereby reduce the voltage loss of the system, and the water management is less critical as well as the heat dissipation.[1,5] The high working temperature, on the other hand, poses practical limitations and restrictions regarding the available polymeric materials for the electrolyte membrane, which can stand the harsh conditions of operating fuel cells. Polybenzimidazole (PBI) membranes doped with phosphoric acid (PA)[9] resulted in an ideal system as polymeric electrolytes thanks to its outstanding thermal stability, good mechanical properties, and proton conductivities, capable of satisfying the stringent U.S. Department Of Energy (DOE) requirements.[4] Proton conduction in PBI−PA membranes has been widely studied also in recent years clarifying the mechanisms behind
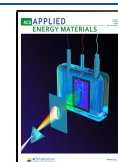
the structural transport (Grotthus mechanism) and the interplay between benzimidazole protonated =N—H sites at the PA molecules.[10−13]

The peculiar hydrogen-bonded (HB) structure together with the high degree of autodissociation of the pure PA is responsible for its unique intrinsic proton diffusion, which is higher than water. The "frustration" of the protons in the PA molecules is strongly perturbed by water and benzimidazole molecules, which causes the conductivity to be much lower in PBI−PA membranes than in anhydrous PA. On the other hand, the interaction of H_3PO_4 with benzimidazole units reduces the hydrophilicity of the acid avoiding excessive swelling and degradation of the HB network and maintaining a high performance even at high doping levels.[10] Different conduction regimes are possible depending on the doping level (PA level) which is defined as the number of PA molecules per repeating unit of PBI. Once the doping level exceeds one molecule of acid per benzimidazole group, the excess of PA molecules compared to the basic nitrogens allows for reconstructing an HB network, which tends to be more similar to pure PA (from PA levels above 4).[8] This explains the proportionality between conductivity and PA doping level and the benefit of incorporating as much PA as possible in PBI−PA systems. The main drawback to this straightforward approach is the deterioration of the mechanical properties of the PBI membrane due to the disruption of the hydrogen bonding between the imidazole rings by the acid and the resulting plasticizing effect.[5,14] Excessive doping also leads to instability problems at high temperatures due to acid leaking with consequent damage to the fuel cell components and a drop in power density/efficiency.[15] To prevent or avoid these problems, different approaches had been attempted. Chemical modification of the commercially available poly [2,2′-m-(phenylene)-5,5′-(bibenzimidazole)] structure was among the first strategies. Modifications of the molecular structure by addition of basic as well as acidic groups were attempted to increase the doping capacity of the membranes.,[5,16−20] Another approach studied was the structural stabilization via blending or copolymerization of polybenzimidazoles.[21−27] Beneficial effects have been obtained also by the addition of free volume elements such as nanoparticles[18,28,29] or by producing porous membranes[30,31] which are capable of stabilizing the PA inside the membrane, limiting both swelling and leaking of the acid. One of the most effective and straightforward strategies to improve the mechanical stability of the PBI−PA membranes at high doping level is covalent cross-linking. The benzimidazole unit can undergo nucleophilic substitution with, for instance, alkyl halides, divinyl sulfone, or epoxides, and this reactivity has been successfully exploited in the past using different types of cross-linkers.[27,32−36] Silicon-based molecules found special appreciation for PEM due to their chemical stability and the possibility to form hybrid networks in situ by sequential modification of the PBI and hydrolysis of the precursors.[37−39] Among those, epoxy-based silanes and siloxanes proved to be an efficient cross-linker, improving doping levels, mechanical properties, and conductivity of PBI−PA hybrid membranes,[14,40−44] Polyhedral oligomeric silsesquioxanes (POSS) are a class of compounds with a well-defined silicon oxide (−Si−O−Si−) rigid core which offers a versatile tool, which has been successfully employed as an additive to improve polymeric protective coatings[45−47] and PEM properties and performances.[48−51] Oxidative stability is another critical issue, which affects the durability and performance of the electrolyte

over time. Thioether (sulfide) containing polymers have particular chemical and oxidative stability as they can act as an effective radical scavenger in oxidative environments limiting polymer degradation.[52−56] In modern times, sulfur is considered a "green" building block because of its excess production from the petrochemical industry.[57] A lot of efforts have been spent to use elemental sulfur for the production of sulfur-rich polymers, because of its low cost and availability, but also trying to fix an environmental issue valorizing a waste and establishing a virtuous (circular) recovery cycle.[58,59]

In this work, we aimed to exploit the chemical stability of aromatic polyphenylene sulfides including a benzimidazole moiety in each repeating unit, successfully obtaining a fully amorphous poly(phenylene sulfide benzimidazole) (PPSBi) with improved solubility in polar aprotic solvents. Freestanding membranes were obtained by casting different PPSBi/glycidyl POSS (g-POSS) solutions and thermally cross-linking the resulting films. The octa-epoxy functionalized g-POSS ensured a high cross-linking density with controlled size and distances within the network. The resulting membranes had good thermal and mechanical properties with excellent oxidative stability. After doping with PA, mechanical strength did not deteriorate, and promising proton conductivity was obtained.

■ EXPERIMENTAL SECTION

Materials. Phosphorus pentoxide (P_2O_5, Acros Organics), phosphoric acid 85 wt % (H_3PO_4, Acros Organics), anhydrous potassium carbonate (K_2CO_3, 99% Acros Organics), methanesulfonic acid (99% Sigma-Aldrich), 3,5-difluorobenzoic acid (3,5-DFBA, >98% TCI Chemical), sodium hydroxide pellets (NaOH, Merck), benzene-1,2-diamine (o-PDA, 99%, TCI Chemical), toluene (99.8% extra dry stored over molecular sieves, water <50 ppm Acros organics), acetone (HPLC grade Macron), absolute ethanol (EtOH, Baker), hydrolyzed trimethoxy[3-(oxiranylmethoxy)propyl]silane (g-POSS) (Hybrid Plastics) were used as received.

N-Methyl-2-pyrrolidone (NMP, 99.5%, extra dry Acros Organics) was distilled from P_2O_5 under vacuum (water content 20 ppm Karl Fischer test); 4,4′-thiobisbenzenethiol (TBBT) (98% Sigma-Aldrich) was recrystallized from toluene.

Synthesis of 2-(3,5-Difluorophenyl) Benzimidazole (DFBi). In a dried 250 mL three-neck round-bottom flask with an argon inlet, a condenser, and a stirring egg, Eaton's reagent was prepared in situ by dissolving 20 g of P_2O_5 into 200 g of methanesulfonic acid under argon. After a clear viscous solution was obtained, 10 g (63.2 mmol) of 3,5-DFBA and 7.18 g (66.4 mmol) of o-PDA were added under argon. The temperature of the oil bath was raised to 120 °C for 15 h.

After cooling down to room temperature, the dark brown solution was slowly poured into an ice−water mixture and then neutralized with a NaOH 15% w/w in water until alkaline pH (8−9) was reached. The product was filtered and washed several times with water until neutrality (pH ≅ 7) in the filtrate was achieved.

The solid was dried in vacuum at 80 °C overnight and then recrystallized from an EtOH:H_2O mixture (3:7 v/v) obtaining fine needlelike crystals, which were washed thoroughly with the cold crystallization mixture and then dried at 80 °C under vacuum for 24 h.

mp 224−226 °C. Anal. Calcd for $C_{13}H_8N_2F_2$: C, 67.82%; H, 3.50%; N, 12.17%. Found: C, 67.75%; H, 3.54%; N, 11.91%. ¹H NMR (400 MHz, DMSO-d_6): δ 13.09 (s, NH), 7.86 (h, J = 4.9 Hz, H_B), 7.70 (d, J = 7.8 Hz, H_C), 7.57 (d, J = 7.8 Hz, H_D), 7.40 (t, J = 9.3, 2.4 Hz, H_A), 7.25 (dt, J = 18.9, 7.1 Hz, 1H_E).

Synthesis of Poly(phenylene sulfide benzimidazole) (PPSBi). To a dried 100 mL three-neck round-bottom flask equipped with an argon inlet, overhead stirrer, and a Dean−Stark trap fitted with a condenser, 1.000 g (4.34 mmol) of 2-(3,5-difluorophenyl) benzimidazole, 1.088 g (4.34 mmol) of 4,4′-thiobisbenzenethiol, and 0.901 g (6.52 mmol) of anhydrous potassium carbonate were added. The solid mixture was solubilized in 10 mL of anhydrous *N*-methyl-2-

pyrrolidone and 5 mL of dry toluene, and the resulting solution was stirred for 10 min at room temperature under an argon atmosphere. The temperature of the oil bath was slowly raised to 150 °C and left distilling out the water for 4 h before raising the temperature to 190 °C and continuing the reaction for 40 h.

The viscous solution was cooled down to room temperature, diluted with 2 mL of dry N-methyl-2-pyrrolidone, and then precipitated in 300 mL of distilled water.

After thoroughly stirring and washing with water, the polymer was dried and reprecipitated from N,N-dimethylformamide in excess acetone. The solid was extensively stirred at room temperature and then recovered by 30 min of centrifugation at 4500 rpm. The collected solid was dried at 80 °C under vacuum for 24 h to give 1.308 g of polymer (68% yield).

^{1}H NMR (400 MHz, DMSO-d_6): δ 6.43 (s), 7.19 (m, 13H), 7.45 (m, 2H), 8.04 (d, 2H), 13.05 (s, 1H).

Membrane Preparation. To a 10 wt % solution of PPSBi in DMSO, a variable amount between 1.5 and 15 wt % (based on PPSBi weight) of g-POSS was added as 10 wt % solution in DMSO and then stirred for 2 h at room temperature. After mixing, the solutions were filtered through a 0.45 μm PTFE filter and drop cast on aluminum plates. The membranes were dried in air at 80 °C for 6 h and successively were heated at 200 °C for 15 h to allow cross-linking of the PPSBi and to evaporate the solvent. The membranes were peeled off in deionized water and then dried for 20 h at 110 °C under vacuum. The resulting cross-linked membranes are indicated as cPPSBi_X (X = 1.5, 3.5, 5, 10, and 15, separately) with X representing the cross-linking content as weight percentage of g-POSS.

Phosphoric Acid (PA) Doping. The membranes were doped in phosphoric acid at 50 °C for 3 h. The excess phosphoric acid was blot dried from the surface and the doped membrane dried under vacuum at 110 °C for 15 h. The PA doping level was evaluated using the weight of the doped dried membrane (w_{doped}) and the weight of the initial dry membrane before doping (w_{dry}) and according to eq 1.

$$PA\ level = \frac{\left[\frac{w_{doped} - w_{dry}}{M_{PA}}\right]}{[w_{dryPPSBi}/M_{PPSBi}]} \quad (1)$$

where M_{PA} is the molecular weight of the phosphoric acid, and M_{PPSBi} is the molecular weight of the PPSBi repeating unit. For the calculation of the PA level of cross-linked membrane, the weight of the dry membrane was corrected for the effective PPSBi content: $w_{dryPPSBi} = w_{dry\text{-}membrane} \times (1 - X)/100$, with X being the weight percentage of cross-linker.

The PA uptake was calculated as the mass increase of the membrane after doping according to eq 2.

$$PA\ uptake\ \% = \frac{(w_{doped} - w_{dry})}{w_{dry}} \times 100 \quad (2)$$

Phosphoric Acid Retention Test. The dried PA doped membranes were hung over boiling water for a period of 5 h, and the weight of the membrane was recorded every hour (w_t) after wiping off the leached acid and condensed water from the membranes. The weight loss ratio of acid in the membranes was calculated according to eq 3.

$$R\ \% = \frac{W_0 - W_t}{W_{PA}} \times 100 \quad (3)$$

where, w_0 is the initial weight of the PA doped membrane, w_t is the weight of the PA doped membrane after leaching at different times, and w_{PA} is the original weight of PA present in the membranes calculated from the PA doping level of the membranes.

Characterization. *Nuclear Magnetic Resonance Spectroscopy (NMR).* NMR spectra were recorded at room temperature using a Varian VXR 400 MHz (^{1}H, 400 MHz; ^{13}C, 100 MHz; ^{19}F, 376 MHz) spectrometer and using CDCl$_3$ and DMSO-d_6 as solvents. Chemical shifts (δ) are reported in ppm and calibrated to the solvents' residual peaks.

Gel Permeation Chromatography (GPC). The molecular weights (M_n number and M_w weight-average molecular weights) and the dispersity (Đ) of the samples were determined by GPC using DMF (containing 0.01 M LiBr) as the solvent in a Viscotek GPCmax instrument equipped with model 302 TDA detectors and two columns (Agilent Technologies-PolarGel-L and M, 8 μm, 30 cm) at a flow rate of 1.0 mL min^{-1} and 50 °C.

Narrow dispersity PMMA standards (Polymer Laboratories) were used for constructing a universal calibration curve, and the Mark–Houwink parameter was applied for determining the molecular weights of the polymers. For sample preparation, the purified dry samples were dissolved in DMF (containing 0.01 M LiBr). Once the samples were completely dissolved, they were filtered through a PTFE syringe filter (Minisart SRP 15, Sartorius stedim biotech, PTFE-membrane filter; pore size, 0.2 μm; filter diameter, 15 mm) and analyzed by GPC using a 100 μL injection volume. The collected spectra were analyzed with the use of an OmniSEC instrument (v5.0) (Malvern).

Attenuated Total Reflection–Fourier Transform Infrared Spectroscopy (ATR–FTIR). Background corrected FTIR spectra were recorded on a Bruker Vertex 70 spectrophotometer in the range 4000–400 cm^{-1}, using 64 scans at a nominal resolution of 4 cm^{-1} using a diamond single reflection attenuated total reflectance (ATR). Atmospheric compensation and offset-correction were applied on the collected spectra with the use of OPUS spectroscopy software (v7.0) (Bruker Optics).

Differential Scanning Calorimetry (DSC). Calorimetric measurements were made on a TA-Instruments Q1000 differential scanning calorimeter under a dry nitrogen atmosphere (50 mL min^{-1}). The samples were scanned in a temperature range from 0 to 250 °C by heating–cooling–heating scans at a heating/cooling rate of 10 °C min^{-1}. The glass transition temperature (T_g) was determined as the inflection point of the specific heat change in the second heating curve. The thermograms were evaluated with the use of TRIOS software (v5.1) (TA Instruments).

Thermogravimetric Analysis (TGA). To determine the thermal stability and decomposition behavior, TGA measurements were performed on a TA-Instruments D2500 device. A programmed heating ramp from 35 to 700 °C was used at a heating rate of 10 °C min^{-1} under nitrogen purge gas (50 mL min^{-1}). The decomposition temperature (T_d) of the samples was assigned to the temperature corresponding to the 5% weight loss of the initial mass. TRIOS software (v5.1) (TA Instruments) was used to analyze the TGA curves.

Oxidative Stability. The chemical stability of the undoped cross-linked and pristine membranes was measured using Fenton's reagent (3% H$_2$O$_2$ aqueous solution containing 2 ppm of Fe^{2+}). The residual weight (RW) was calculated by the difference of the weight of the membrane before and after 1 h of immersion in Fenton's reagent at 80 °C. The oxidative stability was evaluated, also extending the immersion in Fenton's reagent and monitoring the weight on a daily basis. Every 24 h, the samples were taken out, washed with Milli-Q water, and dried at 110 °C under vacuum for 15 h before weighting. The samples were then immersed again in fresh Fenton's reagent for continuing the test.

Tensile Test. Mechanical properties of the membranes were tested on an Instron Model IX 5565 instrument with a 100 kN load cell at ambient conditions (25 °C and RH 45 ± 5%) with a strain speed of 1 mm min^{-1} and membrane size of 25 × 4 mm.

Electrochemical Impedance Spectroscopy (EIS). Ion conductivity of the doped membrane was measured by four-electrode AC electrochemical impedance spectroscopy using an SP300 potentiostat (Bio-Logic) equipped with a controlled environment sample holder (CESH, Bio-Logic). The membranes were dried 24 h at 110 °C under vacuum before each measurement. Proton conductivity was measured in the frequency range from 1 MHz to 10 Hz with an AC voltage amplitude of 50 mV against a 0 V bias DC. The temperature was controlled with a thermocouple placed on the top support of the membrane with an accuracy of ±1 °C while the CESH was heated via a heating plate and insulated with a custom-made insulating mantle to

Scheme 1. (a) Synthesis of the Poly(phenylene sulfide benzimidazole) (PPSBi) and (b) Scheme for the Preparation and Structures of the Cross-Linked cPPSBi_X Networks[a]
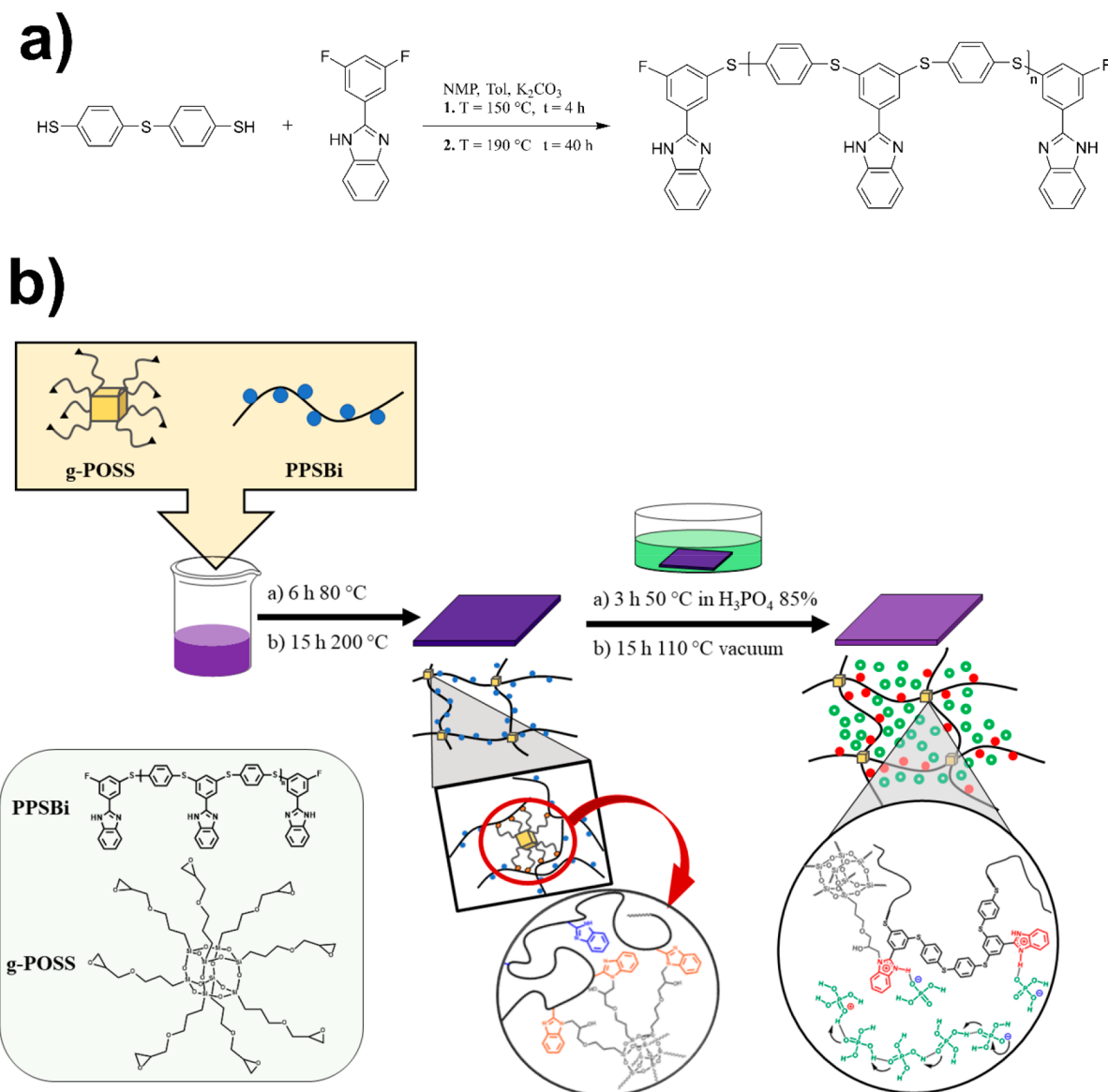
[a]In the first step, the PPSBi (black line with blue dots) is cross-linked with the g-POSS (yellow cubes) to give the cPPSBi. The orange color has been used to identify the nonprotonated cross-linked benzimidazole groups while the nonprotonated free benzimidazoles are colored in blue. In the last step, after the doping with phosphoric acid (PA, green), benzimidazolium ions are formed (red), and the cross-linked network hosts the excess PA molecules responsible for the proton conduction mechanism, schematically represented in the bottom right zoom lens.

minimize heat dispersions. The measurement was performed upon heating from 100 to 180 °C feeding current with two outer electrodes and measuring the voltage drop between the two inner electrodes. The proton conductivity was calculated according to eq 4:

$$\sigma = \frac{1}{R_b A}$$

$$(4)$$

Here, l is the distance between the sensing electrodes (1 cm), R_b is the membrane resistance, and A is the cross-sectional area of the membrane.

Small Angle X-ray Scattering (SAXS) Analysis. X-ray measurements were conducted using the Multipurpose Instrument for Nanostructure Analysis (MINA) diffractometer in Groningen equipped with a Cu rotating anode ($\lambda = 1.5413$ Å). The sample-to-detector distance was 3 m, and the SAXS patterns were collected using a Bruker Vantec2000 detector with a pixel size of 68 μm × 68

μm. The direct beam position and the scattering angle scale were calibrated using a standard silver behenate powder. The SAXS patterns were converted into the one-dimensional scattering intensity profiles by radial azimuthal integration using Fit2D software. The scattering intensity profiles are plotted as a function of the modulus of the scattering vector $q = 4\pi \sin(\theta)/\lambda$ where θ is half of the scattering angle.

■ RESULTS AND DISCUSSION

Synthesis and Characterization. The synthetic route to obtain the PPSBi polymer is summarized in Scheme 1a. The novel monomer 2-(3,5-difluoro)benzimidazole (DFBi) used for the synthesis of the PPSBi polymer was synthesized using a modified procedure reported in the literature (Scheme S1).[60] The successful synthesis of the DFBi monomer was confirmed

by NMR and FTIR spectroscopy (Figures S1 and S2). The ^{1}H NMR signals clearly show the aromatic protons between 7 and 8 ppm and the −NH− signal at 13.25 ppm of the imidazole ring. The composition of the monomer was further confirmed by elemental analysis and the narrow melting point between 224 and 226 °C. The DFBi monomer was employed in the aromatic substitution polymerization of the poly(phenylene sulfide benzimidazole) together with TBBT as the comonomer and potassium carbonate. To maximize the molecular weight, an equimolar amount of the two monomers was used, together with an extended reaction time of 40 h in NMP as solvent. According to GPC analysis, the resulting polymer reached a molecular weight (M_w) of 19.2 kg mol^{-1} with a Đ of 3.2. Fluorine end-groups were detected by ^{19}F NMR analysis indicating DFBi functionalities at the end of the polymer chains. The ^{1}H NMR spectrum (Figure 1a) shows all the aromatic peaks of the polymer backbone and a small signal at 6.43 ppm belonging to the proton of the phenyl ring of the DFBi end-groups, which was used to estimate the molecular weight by NMR. The theoretical value was in good agreement with the result obtained by GPC analysis (Table S1).
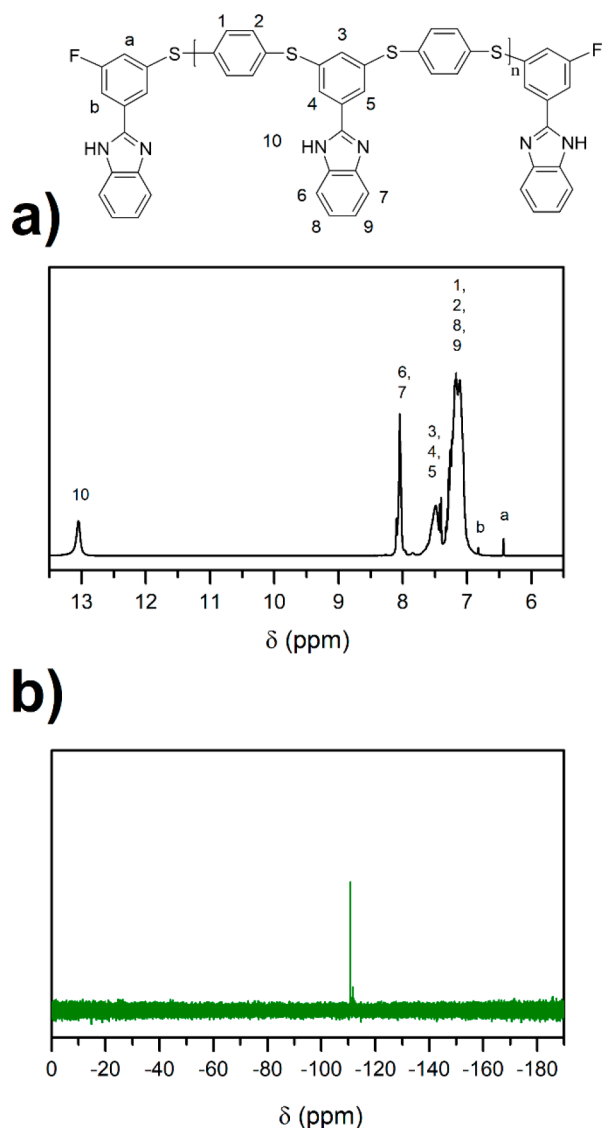

Figure 1. (a) ^{1}H NMR and (b) ^{19}F NMR spectra of the PPSBi.

Low-molecular-weight PBI proved to perform better in MEA,[61] and different structures have been also designed to improve solubility and filmability.[16,18] The PPSBi obtained here had excellent solubility in polar aprotic solvents with its relatively not too large molecular weight, but its filmability was poor. In order to produce high-quality, mechanically robust, freestanding membranes, we have explored a cross-linking strategy that used a multifunctional g-POSS as the cross-linking motif (see Scheme 1b). POSS molecules indeed have been demonstrated to have beneficial effects when included in polymer composites endowing the resulting materials with high resistance toward several environmental degradation factors, such as moisture, oxidation, corrosion, and UV radiation.[62]

The chemical structures of the polymer and the cross-linked membranes were studied via FTIR (Figure 2). For all the samples, FTIR analysis showed a broad band absorption between 2400 and 3500 cm^{-1} which contains the stretching vibrations of the aromatic C—H bond together with the N—H stretching above 3000 cm^{-1} and the absorption of the hydrogen bonding between the imino and amino groups in the region 2800−2600 cm^{-1}. The p-phenylene sulfide moieties appeared as typical signals of poly(p-phenylene sulfides)[63] at 1570, 1471, 1093, 1074, 811, and 480 cm^{-1}, while the benzimidazole unit gave the characteristic C=N stretching at 1520 cm^{-1}, together with the in-plane deformation of the imidazole ring at 1440 cm^{-1} and the C—N stretching vibration at 1280 cm^{-1}.[40] In addition to the aforementioned bands, cPPSBi_X membranes exhibited additional signals belonging to the g-POSS, namely, the bending vibrations of the Si—C bending at 1200 cm^{-1} and the C—H stretching of the aliphatic chain at 2855 cm^{-1}. The intensity of these two absorption bands increased proportionally with the amount of cross-linker. On the other hand, the epoxy peak at 910 cm^{-1} of the glycidyl units disappeared in all the membranes demonstrating successful cross-linking.

Thermal Properties. The thermal properties of the novel polymeric material and the cross-linked networks were studied via DSC and TGA. The results are summarized in Table S2.

The T_g of the pristine PPSBi is 207.5 °C, well below the T_g of neat PBI;[64] more interestingly, also the cross-linked network showed a similar T_g (Figure S4b). This effect is well-known for hybrid composites involving POSS cross-linker, and it can be ascribed to the balance between the bulky size of the cross-linker and the rigidity induced by the cross-linking.[47]

Both the PPSBi polymer and the cPPSBi_X membranes showed high thermal stability with decomposition temperatures T_d above 400 °C. The initial mass decrease for the membrane with X < 10 between 200 and 300 °C is due to evaporation of some residual DMSO strongly bound to the network, similar to what was reported for DMAc[36] (Figure 3a). An additional test in an air atmosphere for the cPPSBi_1.5 membrane was performed to verify the impact of oxidant atmosphere on the degradation process. The thermogram is reported in Figure S5. An identical trend for the T_d is observed, while a two-step process is observed in air because of the complete oxidation of the PPSBi starting around 600 °C. The doped membranes showed good thermal stability up to 240 °C which is above the temperature range for HT-PEMFC (100−200 °C). The first step in the thermograms belongs to the conversion of PA into pyrophosphoric acid.[65] A second step at 380 °C indicates the degradation of the cross-linker followed by the decomposition of the backbone (Figure 3b).
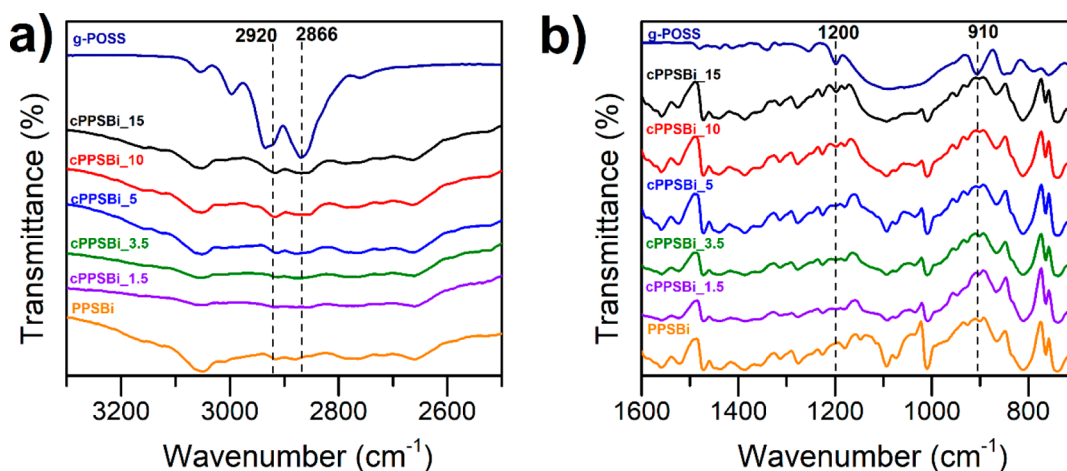
Figure 2. FTIR spectra of the pristine PPSBi, g-POSS, and cPPSBi_X membranes. (a) Aliphatic C−H stretching of the g-POSS at 2886 cm^{-1} appeared in the cross-linked membrane together with the Si−C bending signal at 1200 cm^{-1}. (b) The disappearance of the epoxy band at 910 cm^{-1} confirms the cross-link reaction with the benzimidazole. The dashed lines are guides for the eyes indicating the position of the peaks representing the incorporation of the g-POSS into the PPSBi matrix.
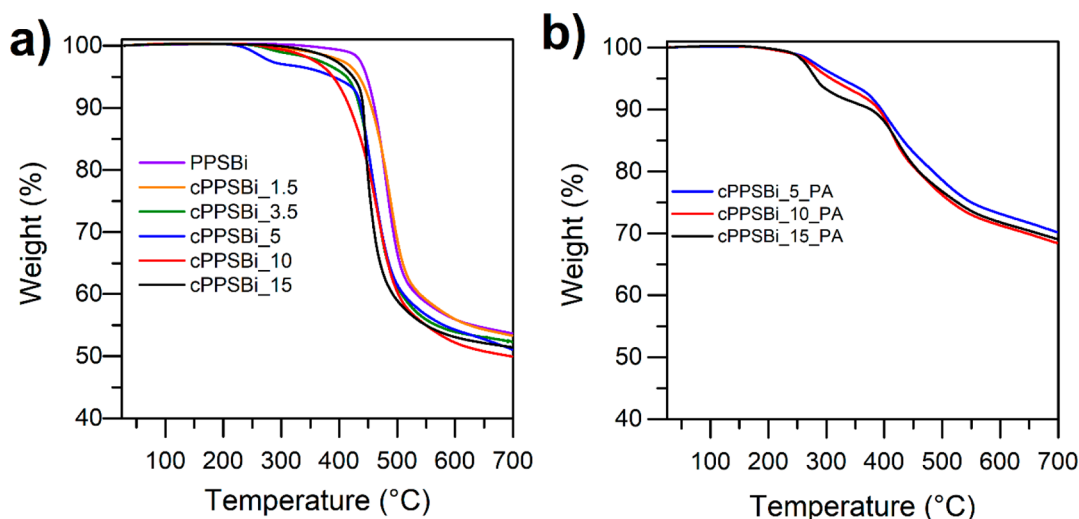

Figure 3. TGA thermograms under a N$_2$ atmosphere of the PPSBi polymer and the cross-linked cPPSBi_X membranes (a) in the undoped state and (b) doped with PA.

Solubility Tests and Network Structure. The solubility of PPSBi and cPPSBi_X membranes was tested in DMAc at 80 °C. The results are summarized in Figure 4a, and they clearly show the effect of the cross-link on the solubilization of the membranes. SAXS analysis provides valuable hints to understand the structure of the cross-linked network at the nanoscale and explaining, at the same time, some features of the solubility behavior (see Figure 4b). The PPSBi polymer does not show any particular features in the probed angular range (probed d-spacing range from 125 to 4 nm), suggesting that the homopolymer is an amorphous, homogeneous physical network. When the cross-linker ratio is between 1.5% and 5%, a broad but measurable signal appears at low q-values (Figure 4b), associated with the formation of some structural inhomogeneities in the cross-linked network. This could be ascribed to the nonhomogeneous distribution of the g-POSS cross-linker within the PPSBi matrix, so that some part of the material may still present low (or even no) cross-linking at the lowest POSS content. This aligned well with the solubility test results, which highlighted the inverse relationship between residual weight and cross-linker ratio.

The density of these cross-linked regions evolved with the cross-linking ratio, as the location of the bump shifts toward high q-values with increasing cross-linking ratio (see inset of Figure 4b). The low-q region can be modeled in order to extract the inhomogeneity correlation length Ξ (related to the average distance between regions with high cross-linking density) using the Debye−Bueche equation:[66]

$$I(q) = \frac{I(0)}{(1 + q^2\Xi^2)^2} + \mathrm{bkg} \tag{5}$$

where $I(0)$ is the asymptotic value of the intensity at $q \rightarrow 0$ of the Debye−Bueche equation, and bkg is the high angle constant background. The solid lines in Figure 4b represent the best fit obtained using eq 5. A decrease of the correlation length is expected when the cross-linking density is increased.[67] The estimated inhomogeneity correlation length was 21.8, 19.0, and 9.5 nm for the films with cross-linking ratios of 1.5%, 3.5%, and 5%, respectively. When the cross-linking ratio is further increased to 10% and 15%, the SAXS profiles do not show any more particular features, suggesting
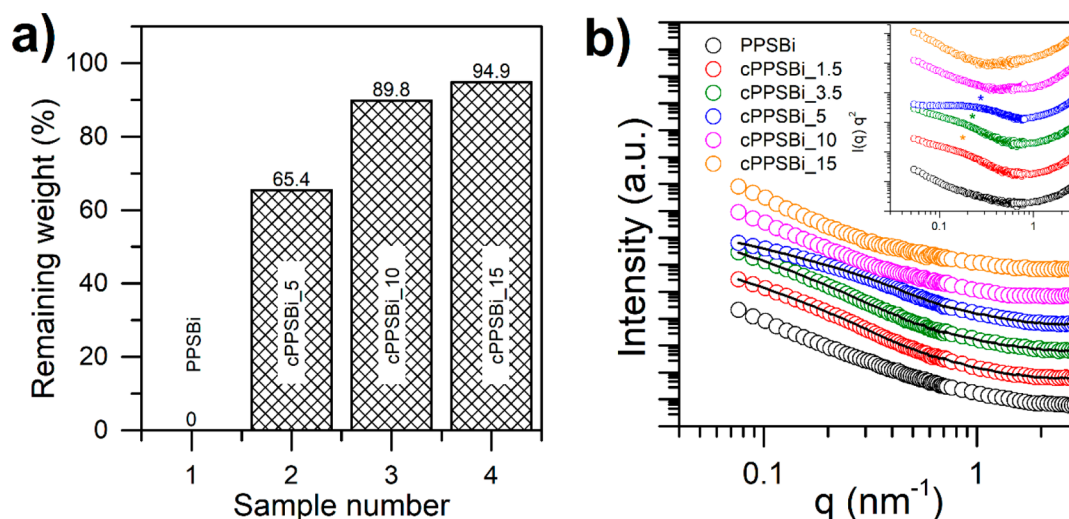
Figure 4. (a) Solubility test results for the PPSBi and cPPSBi_*X* membranes. (b) SAXS curves of the cPPSBi_*X* network at different cross-linking densities. The $I(q)q^2$ vs q plots are reported in the inset. The * symbol indicates the location of the low-q intensity bump generated from the scattering of inhomogeneities in the networks. The black solid lines are the best fits using eq 5.

that for these two samples the cross-linking is homogeneously distributed in the probed angular range. The solubility of the cPPSBi_10 and cPPSBi_15 in DMAc is strongly reduced especially considering that the PPSBi is very soluble in the same solvent and dissolves even at room temperature within a few minutes.

Phosphoric Acid Doping. The phosphoric acid (PA) doping was studied by immersing in phosphoric acid 85 wt % the three samples that provided membranes with the best quality, namely, the cPPSBi_5, cPPSBi_10, and cPPSBi_15. When immersed in the PA solution, the cPPSBi_5 membrane lost its dimensional stability even at low doping level, and it was discarded from further tests. A 48 h doping test at room temperature for the cPPSBi_10 and cPPSBi_15 membranes resulted in only 20% PA uptake. Doping at higher temperature yielded higher uptake in a sensibly shorter time (see Figure S6a). A doping temperature of 50 °C was found to give the best compromise between fast PA uptake and dimensional stability retention. Doping the membranes at higher temperature ($T = 60$ °C) induced PA uptakes >150% with subsequent loss of mechanical stability. The final PA uptake values were 113% for the cPPSBi_10 and 90% for the cPPSBi_15, which corresponded to a PA level of 5.6 and 4.8, respectively (Figure S6b). It is important to note that, by definition, the PA level refers to the moles of PA per repeating unit of the polymer, besides the effective content of benzimidazole units. In our case each repeating unit contains only one benzimidazole, meaning that a PA level of 5 corresponds to a PA level of 10 for a conventional PBI. The molecular design of the PPSBi polymer and the cross-linked networks was meant to facilitate the accessibility of the benzimidazole functionality aiding the doping with PA but without losing mechanical stability thanks to the dense cross-linking network. This is thanks to the pendant position of the benzimidazole groups and the free volume associated with the POSS particles. The positive effect of this approach resulted in a lower T_g of the pristine polymer and the polymer networks compared to classical PBI[64] and also in a faster PA uptake at moderate temperature compared to other works.[35,51,65] Moreover, we have exposed the doped membranes in a water vapor atmosphere at 100 °C for 5 h in order to verify the PA retention ability of our materials (see

Figure S7). We found that our membranes exhibit an approximately 20% PA retention that is much higher than reference OPBI. However, this value is not as high as the one reported for m-PBI probably due to the lower content of benzimidazole in our PPSBi and the possible location of part of the PA molecules in the free volume of the polymer matrix. We must note that the PA retention ability of our materials may be also limited by the low molecular weight achieved here. Increasing the molecular weight of the pristine PPSBi and further optimization of the degree of cross-linking, consequently strengthening the interchain interactions, are expected to improve the PA retention properties of our cPPSBi_*X* membranes. These aspects are currently under investigation in our group

Mechanical Properties. The mechanical properties of the cPPSBi_10 and cPPSBi_15 membranes were evaluated by tensile tests, and the results are summarized in Table 1. The

Table 1. Summary of the Tensile Properties of Undoped and Doped cPPSBi_*X* Membranes

sample	stress at break (MPa)		elongation at break (%)		Young's modulus (MPa)	
	undoped	doped[a]	undoped	doped[a]	undoped	doped[a]
cPPSBi_10	5.9	2.3	1.6	3.1	598	59
cPPSBi_15	12.7	4.6	2.1	2.2	868	317

[a]The doped samples had a PA uptake of 90%.

neat polymer, as well as all the cross-linked membranes with g-POSS content below 10%, could not be tested due to the poor film-forming behavior. The sulfide structure of the backbone is rigid and provides stiffness to the resulting material, similar to what was reported for aliphatic thioether containing benzimidazole.[52] The cPPSBi_10 and cPPSBi_15 stress—strain curves (Figure S8) revealed the rigid structure of the membranes with low strain at break and high modulus (868 MPa for cPPSBi_15). We noticed that the elastic modulus is lower when compared to values reported for classical PBI membranes, which are in the range of units of GPa, and this can be explained considering the lower density and different position of the benzimidazole units in the polymer backbone,
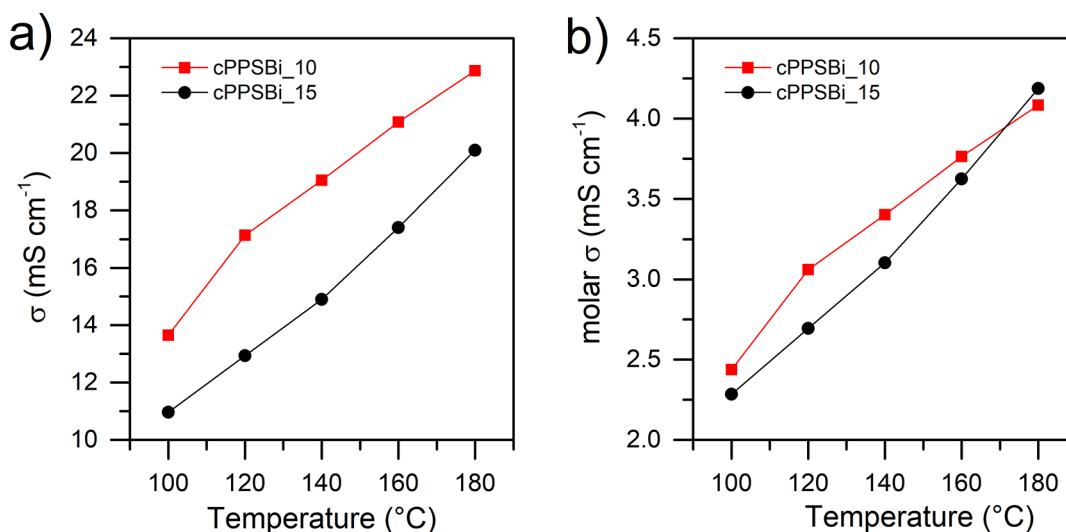
Figure 5. (a) Proton conductivity of cPPSBi_10 and cPPSBi_15 as a function of temperature and (b) normalized conductivity for the PA molecule in the cross-linked network.

which enable the formation of fewer hydrogen bonds between the benzimidazole moieties. The higher content of g-POSS in cPPSBi_15 is responsible for an approximately 2 times higher stress at break with respect to the cPPSBi_10 due to the higher number of interconnections between the polymer chains. Additionally, the low molecular weight of the polymer and its high density of cross-linking compared to similar systems[68] negatively affect the tensile strength of the produced membranes. What is encouraging is the behavior of cross-linked membranes in the doped state. The PA doping inevitably affected the mechanical properties due to the breakdown of the intermolecular forces, namely, the hydrogen bonding between —C=N— and —NH— groups of the imidazole rings. As a consequence, the stress at break and the modulus of the doped membrane significantly decreased compared to the undoped membranes. The values reported in Table 1 show a neat difference between the stress at break of the doped membranes which is more than halved compared to the related undoped ones. However, the value of about 300 MPa measured for the cPPSBi_15 membrane was more than 5 times higher in comparison to PBI−PA membranes with a similar cross-linking density and similar doping level, which reports a Young's modulus of 40 MPa.[40] The lower drop can be explained again in terms of the different molecular design but also considering the structure of the POSS cage and the relatively short branches of the glycidyl units which build up a homogeneous network as demonstrated also via X-ray analysis (vide infra). The limited size of the cage and the high number of functionalities enable the membrane standing a high level of PA doping and avoiding degradation of the mechanical properties. The stress at break is also in the range 2−5 MPa which is considered useful for conducting fuel cell performance tests.[20]

Proton Conductivity. Proton conduction in PBI−PA doped membranes under anhydrous conditions is known to happen through structural diffusion (Grotthus mechanism). Proton transfer mainly involves phosphate ions while the benzimidazolium cations are excluded from the conduction mechanism due to slower proton exchange between benzimidazoles and phosphoric acid compared to proton exchange between phosphate species.[8,13,69] The proton

conductivity of the doped dry membranes was tested in the range 100−180 °C, and the results are reported in Figure 5. We recall that cPPSBi_10 has a PA level of 5.6, while the cPPSBi_15 has 4.8 due to the different PA uptake (Figure S6a). The proton conductivity increased proportionally with the PA level of the membrane with cPPSBi_10 reaching a maximum conductivity of 23 mS cm^{-1} (Figure 5a), which is suitable for use as PEM.[52,70] When looking at the molar conductivity (conductivity divided by the PA level) as a function of temperature, the difference in transport behavior between the two membranes is almost negligible (Figure 5b), with the cPPSBi_15 membrane holding better the conductivity at the highest temperature. The similar behavior observed here for the normalized conductivity of the two membranes could be ascribed to the proton conduction in a PA percolated system, since for membranes with a PA level above 3, the PA domains can be considered percolated.[30] The values of the molar conductivity of cPPSBi are lower than PBI with a similar doping level.[17] This can be explained if we consider the possible interference of the cross-linking to the free proton diffusion in the matrix. Indeed, the cPPSBi_10 and cPPSBi_15 membranes have a nominal molar degree of cross-linking of 29% and 46%, respectively, which created a dense, homogeneous network (as observed by SAXS data discussed above). The dense cross-linking level present in our membranes most probably hinders the free movement of the proton through a PA percolated network. On the other hand, this dense and robust network structure is beneficial to retain higher conductivity at high temperature, as demonstrated by the molar proton conductivity of the cPPSBi_15 membrane that does not decrease with increasing temperature (see Figure 5b). This observation aligns well to the expected benefits from the cross-linking approach which enables higher PA uptake preserving dimensional stability and avoiding PA loss.[10]

The rigid structure of the PPSBi backbone together with the high cross-linking density generate a stiff network which is not easily deformable. These observations explain the increase of the activation energy with cross-linking of the membranes as obtained from the Arrhenius plot (Figure 6) according to eq 6:
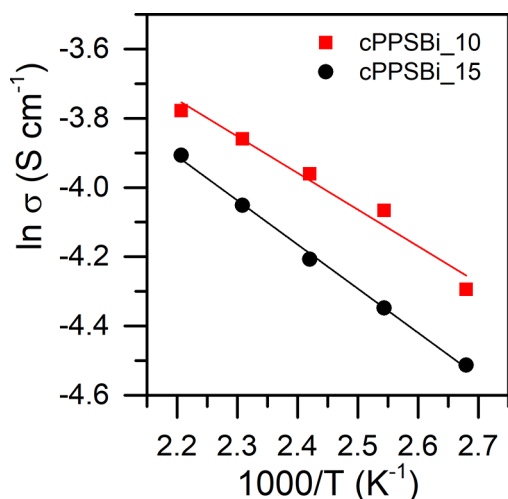
$$\ln \sigma = \sigma_0 - \frac{E_a}{RT} \tag{6}$$

Figure 6. Arrhenius plot of cPPSBi_10 and cPPSBi_15.

The membrane follows in good agreement an Arrhenian behavior showing a linear trend of the conductivity with temperature on a semilogarithmic scale. The higher the degree of cross-link, the higher the activation energy due to the hindrance of the dense network to the free motion of the acid. The values obtained (ca. 10 kJ mol^{-1}) are comparable to reported values for percolated membranes containing sulfides bonds.[52]

Oxidative Stability. The oxidation test was conducted in Fenton's reagent (H_2O_2 3% and Fe^{2+} 2 ppm) at 80 °C immersing the membrane in the solution and checking the weight loss daily. The residual weight (RW) was evaluated after a 1 h test, and the results are reported in Table S2. The PPSBi backbone was designed to implement a high amount of sulfide functionalities to improve the oxidative stability of the resulting material according to beneficial effects previously reported.[52] Additionally, according to the proposed mechanism for PBI oxidative degradation in aqueous media, the cross-linking of the −NH− groups reduces the available number of protons susceptible to abstraction by the hydroxyl radical.[71,72] The polymer and the cross-linked membrane

revealed exceptional oxidative stability with cPPSBi_10 and cPPSBi_15 showing a weight loss of less than 5% after 264 h of immersion in Fenton's reagent at 80 °C much lower than the reference m-PBI (Figure 7a). The sometimes positive variation in the weight might be explained also considering the incorporation of oxygen atoms in the backbone due to the formation of the sulfoxide and sulfone group as a consequence of the oxidation of the thioether functionalities. The different behavior of the PPSBi and cPPSBi_5 explained the crucial role of the g-POSS network in stabilizing the membrane. The missing or incomplete network in PPSBi a cPPSBi_5 (see X-ray results below) does not prevent the penetration and the disruption of the membrane structure, whereas the highly cross-linked membranes are more resistant to oxidative attack, and the time needed to degrade the organic material is sometimes longer than the time needed to oxidize the sulfur moieties.

Macroscopically, the PPSBi membrane broke within the first 48 h while the cPPSBi_5 and cPPSBi_10 cracked at 120 and 264 h, respectively (see Figure S9). FTIR analysis of the samples after the test clearly shows the transformation of the thioether functionality into both sulfoxide and sulfone moieties (Figure 7b). The presence of the characteristic double absorption of the sulfone scissoring at 1324 and 1157 cm^{-1} is accompanied by the appearance of the sulfoxide stretching vibration at 1040 cm^{-1} and the disappearance or reduction of the bands at 480 and 811 cm^{-1} belonging to the p-phenylene sulfide moieties as reported in Figure 2b. Some degradation occurs also for the g-POSS moiety as shown by the almost disappearance of the broad band at 1100 cm^{-1} belonging to the Si−O−Si and to the ether (C−O−C) stretching. The 4,5-disubstituted imidazole ring vibration at 616 cm^{-1} is representative of the scission of the bond with the glycidyl chain of g-POSS which gave a weak shoulder at 640 cm^{-1} in the cross-linked membrane.

CONCLUSIONS

A novel poly(phenylene sulfide benzimidazole) polymer (named PPSBi) has been successfully synthesized through nucleophilic aromatic substitution polymerization. The poly-
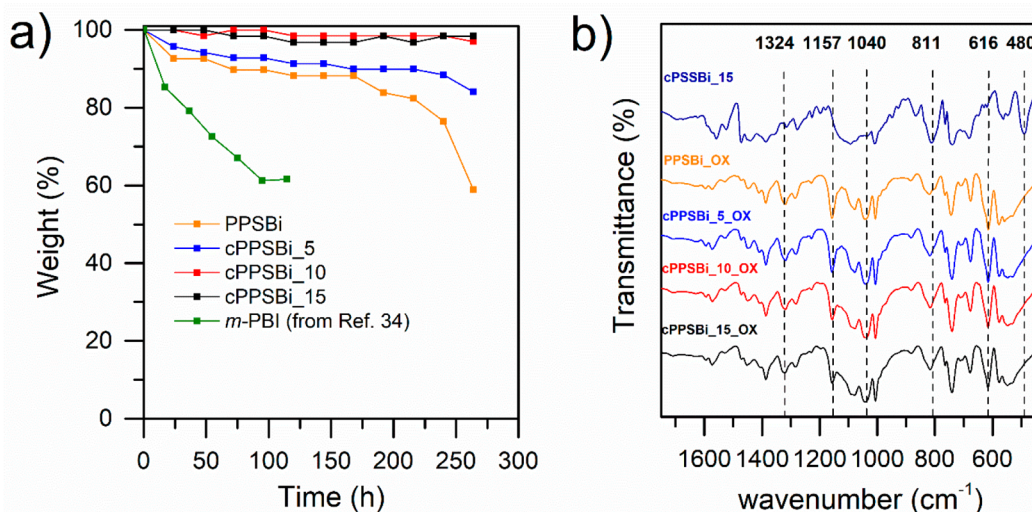

Figure 7. (a) Weight variation of the samples during the oxidation test in Fenton's reagent at 80 °C; values of a conventional m-PBI are reported for comparison from ref 34. (b) FTIR of the samples after 264 h.

mer has a high sulfur content and contains side benzimidazole groups useful for phosphoric acid doping and proton conductivity in high-temperature anhydrous conditions. Drawbacks such as the brittle behavior and the poor filmability of the PPSBi polymer were overcome by network formation using polyfunctional g-POSS cross-linking via benzimidazole-epoxy thermal reaction. The use of g-POSS as a cross-linker ensured the formation of homogeneous, insoluble networks with good dimensional stability, especially in the doped state. The free volume created by the bulky structure of the POSS cage and the branched epoxy functionalities endowed also fast acid uptake at mild conditions without extreme loss of thermal or mechanical properties. Phosphoric acid levels as high as 5.6 PA molecules per benzimidazole group were reached without loss of mechanical and dimensional stability. All the membranes showed good thermal stability with degradation temperatures well above 160 °C, the reference operative temperature for HT-PEMFC.[9,12] When a sufficiently high cross-linking degree is used, membranes of good mechanical stability with high modulus even in the doped state were prepared, confirming the synergic role of the rigid backbone with the nanosized flexible cross-linker. The proton conductivity reached by the membranes (>20 mS cm^{-1}) is promising and comparable to conventional PBI−PA systems with a similar doping level.[40] The most interesting feature exhibited by these novel materials was the high chemical stability. The high sulfide content endowed exceptional oxidative stability with sulfur atoms acting as an effective radical scavenger and g-POSS avoiding excessive swelling and penetration of the oxidant molecules through the membrane. The encouraging results obtained in this work provide insights for future improvements especially by increasing the molecular weight of the constituting PPSBi polymer, obtaining high-quality large-scale membranes, and performing tests in HT-PEMFC.

■ ASSOCIATED CONTENT

ⓈI Supporting Information

The Supporting Information is available free of charge at https://pubs.acs.org/doi/10.1021/acsaem.0c01285.

> ^{1}H, ^{13}C, and ^{19}F NMR of DFBi; FTIR spectrum of the DFBi; GPC trace of PPSBi; DSC traces; structural and thermal property data; TGA thermogram; tensile test graph; PA retention test; and pictures of the membranes during oxidation tests (PDF)

■ AUTHOR INFORMATION

Corresponding Author

Giuseppe Portale − *Macromolecular Chemistry and New Polymeric Materials, Zernike Institute for Advanced Materials, University of Groningen, 9747AG Groningen, The Netherlands;* ⊙ orcid.org/0000-0002-4903-3159; Email: g.portale@rug.nl

Authors

Marco Viviani − *Macromolecular Chemistry and New Polymeric Materials, Zernike Institute for Advanced Materials, University of Groningen, 9747AG Groningen, The Netherlands*

Sebastiaan Pieter Fluitman − *Macromolecular Chemistry and New Polymeric Materials, Zernike Institute for Advanced Materials, University of Groningen, 9747AG Groningen, The Netherlands*

Katja Loos − *Macromolecular Chemistry and New Polymeric Materials, Zernike Institute for Advanced Materials, University of Groningen, 9747AG Groningen, The Netherlands;* ⊙ orcid.org/0000-0002-4613-1159

Complete contact information is available at:
https://pubs.acs.org/10.1021/acsaem.0c01285

Author Contributions

The manuscript was written through contributions of all authors. All authors have given approval to the final version of the manuscript.

Notes

The authors declare no competing financial interest.

■ REFERENCES

(1) Zhang, J.; Xiang, Y.; Lu, S.; Jiang, S. P. High Temperature Polymer Electrolyte Membrane Fuel Cells for Integrated Fuel Cell - Methanol Reformer Power Systems: A Critical Review. *Adv. Sustain. Syst.* **2018**, *2* (8−9), 1700184.

(2) Quartarone, E.; Angioni, S.; Mustarelli, P. Polymer and Composite Membranes for Proton-Conducting, High-Temperature Fuel Cells: A Critical Review. *Materials* **2017**, *10* (7), 687.

(3) Ma, C.; Zhang, L.; Mukerjee, S.; Ofer, D.; Nair, B. An Investigation of Proton Conduction in Select PEM's and Reaction Layer Interfaces-Designed for Elevated Temperature Operation. *J. Membr. Sci.* **2003**, *219* (1−2), 123−136.

(4) Rosli, R. E.; Sulong, A. B.; Daud, W. R. W.; Zulkifley, M. A.; Husaini, T.; Rosli, M. I.; Majlan, E. H.; Haque, M. A. A Review of High-Temperature Proton Exchange Membrane Fuel Cell (HT-PEMFC) System. *Int. J. Hydrogen Energy* **2017**, *42* (14), 9293−9314.

(5) Asensio, J. A.; Sánchez, E. M.; Gómez-Romero, P. Proton-Conducting Membranes Based on Benzimidazole Polymers for High-Temperature PEM Fuel Cells. A Chemical Quest. *Chem. Soc. Rev.* **2010**, *39*, 3210−3239.

(6) Li, Q.; He, R.; Jensen, J. O.; Bjerrum, N. J. Approaches and Recent Development of Polymer Electrolyte Membranes for Fuel Cells Operating above 100 °C. *Chem. Mater.* **2003**, *15* (26), 4896−4915.

(7) Li, Q.; He, R.; Gao, J.-A.; Jensen, J. O.; Bjerrum, N. J. The CO Poisoning Effect in PEMFCs Operational at Temperatures up to 200°C. *J. Electrochem. Soc.* **2003**, *150* (12), A1599.

(8) Ma, Y.-L.; Wainright, J. S.; Litt, M. H.; Savinell, R. F. Conductivity of PBI Membranes for High-Temperature Polymer Electrolyte Fuel Cells. *J. Electrochem. Soc.* **2004**, *151* (1), A8.

(9) Wainright, J. S.; Wang, J.-T.; Weng, D.; Savinell, R. F.; Litt, M. Acid-Doped Polybenzimidazoles: A New Polymer Electrolyte. *J. Electrochem. Soc.* **1995**, *142* (7), L121.

(10) Melchior, J. P.; Majer, G.; Kreuer, K. D. Why Do Proton Conducting Polybenzimidazole Phosphoric Acid Membranes Perform Well in High-Temperature PEM Fuel Cells? *Phys. Chem. Chem. Phys.* **2017**, *19* (1), 601−612.

(11) Melchior, J. P.; Kreuer, K. D.; Maier, J. Proton Conduction Mechanisms in the Phosphoric Acid-Water System ($H_4P_2O_7$-H_3PO_4·$2H_2O$): A ^{1}H, ^{31}P, and ^{17}O PFG-NMR and Conductivity Study. *Phys. Chem. Chem. Phys.* **2017**, *19* (1), 587−600.

(12) Kreuer, K.-D. Ion Conducting Membranes for Fuel Cells and Other Electrochemical Devices. *Chem. Mater.* **2014**, *26* (1), 361−380.

(13) Vilčiauskas, L.; Tuckerman, M. E.; Bester, G.; Paddison, S. J.; Kreuer, K.-D. The Mechanism of Proton Conduction in Phosphoric Acid. *Nat. Chem.* **2012**, *4* (6), 461−466.

(14) Yang, J.; Gao, L.; Wang, J.; Xu, Y.; Liu, C.; He, R. Strengthening Phosphoric Acid Doped Polybenzimidazole Membranes with Siloxane Networks for Using as High Temperature Proton Exchange Membranes. *Macromol. Chem. Phys.* **2017**, *218* (10), 1700009.

(15) Li, Q.; He, R.; Jensen, J. O.; Bjerrum, N. J. PBI-Based Polymer Membranes for High Temperature Fuel Cells− Preparation, Characterization and Fuel Cell Demonstration. *Fuel Cells* **2004**, *4* (3), 147−159.

(16) Li, X.; Wang, P.; Liu, Z.; Peng, J.; Shi, C.; Hu, W.; Jiang, Z.; Liu, B. Arylether-Type Polybenzimidazoles Bearing Benzimidazolyl Pendants for High-Temperature Proton Exchange Membrane Fuel Cells. *J. Power Sources* **2018**, *393*, 99−107.

(17) Yang, J.; Aili, D.; Li, Q.; Xu, Y.; Liu, P.; Che, Q.; Jensen, J. O.; Bjerrum, N. J.; He, R. Benzimidazole Grafted Polybenzimidazoles for Proton Exchange Membrane Fuel Cells. *Polym. Chem.* **2013**, *4* (17), 4768−4775.

(18) Quartarone, E.; Mustarelli, P. Polymer Fuel Cells Based on Polybenzimidazole/H$_3$PO$_4$. *Energy Environ. Sci.* **2012**, *5* (4), 6436−6444.

(19) Peron, J.; Ruiz, E.; Jones, D. J.; Rozière, J. Solution Sulfonation of a Novel Polybenzimidazole: A Proton Electrolyte for Fuel Cell Application. *J. Membr. Sci.* **2008**, *314* (1−2), 247−256.

(20) Xiao, L.; Zhang, H.; Jana, T.; Scanlon, E.; Chen, R.; Choe, E. W.; Ramanathan, L. S.; Yu, S.; Benicewicz, B. C. Synthesis and Characterization of Pyridine-Based Polybenzimidazoles for High Temperature Polymer Electrolyte Membrane Fuel Cell Applications. *Fuel Cells* **2005**, *5* (2), 287−295.

(21) Wang, L.; Liu, Z.; Ni, J.; Xu, M.; Pan, C.; Wang, D.; Liu, D.; Wang, L. Preparation and Investigation of Block Polybenzimidazole Membranes with High Battery Performance and Low Phosphoric Acid Doping for Use in High-Temperature Fuel Cells. *J. Membr. Sci.* **2019**, *572*, 350−357.

(22) Venugopalan, G.; Chang, K.; Nijoka, J.; Livingston, S. M.; Geise, G. G.; Arges, C. Stable and Highly Conductive Polycation− Polybenzimidazole Membrane Blends for Intermediate Temperature Polymer Electrolyte Membrane Fuel Cells. *ACS Appl. Energy Mater.* **2020**, *3* (1), 573−585.

(23) Yang, J.; Li, Q.; Cleemann, L. N.; Jensen, J. O.; Pan, C.; Bjerrum, N. J.; He, R. Crosslinked Hexafluoropropylidene Polybenzimidazole Membranes with Chloromethyl Polysulfone for Fuel Cell Applications. *Adv. Energy Mater.* **2013**, *3* (5), 622−630.

(24) Sana, B.; Jana, T. Polymer Electrolyte Membrane from Polybenzimidazoles: Influence of Tetraamine Monomer Structure. *Polymer* **2018**, *137*, 312−323.

(25) Kerres, J.; Ullrich, A.; Meier, F.; Häring, T. Synthesis and Characterization of Novel Acid−Base Polymer Blends for Application in Membrane Fuel Cells. *Solid State Ionics* **1999**, *125* (1−4), 243−249.

(26) Kerres, J. A. Development of Ionomer Membranes for Fuel Cells. *J. Membr. Sci.* **2001**, *185* (1), 3−27.

(27) Kerres, J.; Atanasov, V. Cross-Linked PBI-Based High-Temperature Membranes: Stability, Conductivity and Fuel Cell Performance. *Int. J. Hydrogen Energy* **2015**, *40* (42), 14723−14735.

(28) Ooi, Y. X.; Ya, K. Z.; Maegawa, K.; Tan, W. K.; Kawamura, G.; Muto, H.; Matsuda, A. CHS-WSiA Doped Hexafluoropropylidene-Containing Polybenzimidazole Composite Membranes for Medium Temperature Dry Fuel Cells. *Int. J. Hydrogen Energy* **2019**, *44* (60), 32201−32209.

(29) Seo, K.; Seo, J.; Nam, K.-H.; Han, H. Polybenzimidazole/Inorganic Composite Membrane with Advanced Performance for High Temperature Polymer Electrolyte Membrane Fuel Cells. *Polym. Compos.* **2017**, *38* (1), 87−95.

(30) Weber, J.; Kreuer, K. D.; Maier, J.; Thomas, A. Proton Conductivity Enhancement by Nanostructural Control of Poly-(Benzimidazole)-Phosphoric Acid Adducts. *Adv. Mater.* **2008**, *20* (13), 2595−2598.

(31) Mecerreyes, D.; Grande, H.; Miguel, O.; Ochoteco, E.; Marcilla, R.; Cantero, I. Porous Polybenzimidazole Membranes Doped with Phosphoric Acid: Highly Proton-Conducting Solid Electrolytes. *Chem. Mater.* **2004**, *16* (4), 604−607.

(32) Aili, D.; Li, Q.; Christensen, E.; Jensen, J. O.; Bjerrum, N. J. Crosslinking of Polybenzimidazole Membranes by Divinylsulfone Post-Treatment for High-Temperature Proton Exchange Membrane Fuel Cell Applications. *Polym. Int.* **2011**, *60* (8), 1201−1207.

(33) Lu, F.; Gao, X.; Dong, B.; Sun, P.; Sun, N.; Xie, S.; Zheng, L. Nanostructured Proton Conductors Formed via in Situ Polymerization of Ionic Liquid Crystals. *ACS Appl. Mater. Interfaces* **2014**, *6* (24), 21970−21977.

(34) Li, Q.; Pan, C.; Jensen, J. O.; Noyé, P.; Bjerrum, N. J. Cross-Linked Polybenzimidazole Membranes for Fuel Cells. *Chem. Mater.* **2007**, *19* (3), 350−352.

(35) Yang, J.; Aili, D.; Li, Q.; Cleemann, L. N.; Jensen, J. O.; Bjerrum, N. J.; He, R. Covalently Cross-Linked Sulfone Polybenzimidazole Membranes with Poly(Vinylbenzyl Chloride) for Fuel Cell Applications. *ChemSusChem* **2013**, *6* (2), 275−282.

(36) Ossiander, T.; Perchthaler, M.; Heinzl, C.; Scheu, C. Influence of Thermal Post-Curing on the Degradation of a Cross-Linked Polybenzimidazole-Based Membrane for High Temperature Polymer Electrolyte Membrane Fuel Cells. *J. Power Sources* **2014**, *267*, 323−328.

(37) Eguizábal, A.; Lemus, J.; Roda, V.; Urbiztondo, M.; Barreras, F.; Pina, M. P. Nanostructured Electrolyte Membranes Based on Zeotypes, Protic Ionic Liquids and Porous PBI Membranes: Preparation, Characterization and MEA Testing. *Int. J. Hydrogen Energy* **2012**, *37* (8), 7221−7234.

(38) Bai, Z.; Rodrigues, S. J.; Dang, T. D. Synthesis and Characterization of Crosslinked Polymer Nanocomposite for Polymer Electrolyte Materials. *J. Membr. Sci.* **2011**, *383* (1−2), 189−196.

(39) Lin, H.; Zhao, C.; Ma, W.; Shao, K.; Li, H.; Zhang, Y.; Na, H. Novel Hybrid Polymer Electrolyte Membranes Prepared by a Silane-Cross-Linking Technique for Direct Methanol Fuel Cells. *J. Power Sources* **2010**, *195* (3), 762−768.

(40) Tian, X.; Wang, S.; Li, J.; Liu, F.; Wang, X.; Chen, H.; Wang, D.; Ni, H.; Wang, Z. Benzimidazole Grafted Polybenzimidazole Cross-Linked Membranes with Excellent PA Stability for High-Temperature Proton Exchange Membrane Applications. *Appl. Surf. Sci.* **2019**, *465*, 332−339.

(41) Yuan, S.; Yan, G.; Xia, Z.; Guo, X.; Fang, J.; Yang, X. Preparation and Properties of Covalently Cross-Linked Sulfonated Poly(Sulfide Sulfone)/Polybenzimidazole Blend Membranes for Fuel Cell Applications. *High Perform. Polym.* **2014**, *26* (2), 212−222.

(42) Hu, M.; Ni, J.; Zhang, B.; Neelakandan, S.; Wang, L. Crosslinked Polybenzimidazoles Containing Branching Structure as Membrane Materials with Excellent Cell Performance and Durability for Fuel Cell Applications. *J. Power Sources* **2018**, *389*, 222−229.

(43) Wang, S.; Zhao, C.; Ma, W.; Zhang, G.; Liu, Z.; Ni, J.; Li, M.; Zhang, N.; Na, H. Preparation and Properties of Epoxy-Cross-Linked Porous Polybenzimidazole for High Temperature Proton Exchange Membrane Fuel Cells. *J. Membr. Sci.* **2012**, *411−412*, 54−63.

(44) Wang, S.; Zhao, C.; Ma, W.; Zhang, N.; Zhang, Y.; Zhang, G.; Liu, Z.; Na, H. Silane-Cross-Linked Polybenzimidazole with Improved Conductivity for High Temperature Proton Exchange Membrane Fuel Cells. *J. Mater. Chem. A* **2013**, *1* (3), 621−629.

(45) Wang, Y.; Liu, F.; Xue, X. Preparation and Properties of UV-Cured Epoxy Acrylate/Glycidyl-POSS Coatings. *J. Coatings Technol. Res.* **2017**, *14* (3), 665−672.

(46) Rodošek, M.; Mihelčič, M.; Čolović, M.; Šest, E.; Šobak, M.; Jerman, I.; Surca, A. K. Tailored Crosslinking Process and Protective Efficiency of Epoxy Coatings Containing Glycidyl-POSS. *Polymers (Basel, Switz.)* **2020**, *12* (3), 591.

(47) Mishra, K.; Singh, R. P. Reinforcement of Epoxy Resins with POSS for Enhancing Fracture Toughness at Cryogenic Temperature. In *Composite Materials and Joining Technologies for Composites, Vol. 7;*

Patterson, E., Backman, D., Cloud, G., Eds.; Springer New York: New York, 2013; pp 179−187.

(48) Liu, C.; Wu, Z.; Xu, Y.; Zhang, S.; Gong, C.; Tang, Y.; Sun, D.; Wei, H.; Shen, C. Facile One-Step Fabrication of Sulfonated Polyhedral Oligomeric Silsesquioxane Cross-Linked Poly(Ether Ether Ketone) for Proton Exchange Membranes. *Polym. Chem.* **2018**, *9* (26), 3624−3632.

(49) Pan, H.; Zhang, Y.; Pu, H.; Chang, Z. Organic−Inorganic Hybrid Proton Exchange Membrane Based on Polyhedral Oligomeric Silsesquioxanes and Sulfonated Polyimides Containing Benzimidazole. *J. Power Sources* **2014**, *263*, 195−202.

(50) Chang, Y.-W.; Shin, G. Crosslinked Poly(Ethylene Glycol) (PEG)/Sulfonated Polyhedral Oligosilsesquioxane (SPOSS) Hybrid Membranes for Direct Methanol Fuel Cell Applications. *J. Ind. Eng. Chem.* **2011**, *17*, 730−735.

(51) Lin, B.; Chu, F.; Yuan, N.; Shang, H.; Ren, Y.; Gu, Z.; Ding, J.; Wei, Y.; Yu, X. Phosphoric Acid Doped Polybenzimidazole/Imidazolium-Modified Silsesquioxane Hybrid Proton Conducting Membranes for Anhydrous Proton Exchange Membrane Application. *J. Power Sources* **2014**, *252*, 270−276.

(52) He, C.; Han, K.-F.; Yu, J.-H.; Zhu, H.; Wang, Z.-M. Novel Anti-Oxidative Membranes Based on Sulfide-Containing Polybenzimidazole for High Temperature Proton Exchange Membrane Fuel Cells. *Eur. Polym. J.* **2016**, *74*, 168−179.

(53) Zhao, D.; Li, J.; Song, M. K.; Yi, B.; Zhang, H.; Liu, M. A Durable Alternative for Proton-Exchange Membranes: Sulfonated Poly(Benzoxazole Thioether Sulfone)S. *Adv. Energy Mater.* **2011**, *1* (2), 203−211.

(54) Shin, D. W.; Lee, S. Y.; Kang, N. R.; Lee, K. H.; Guiver, M. D.; Lee, Y. M. Durable Sulfonated Poly(Arylene Sulfide Sulfone Nitrile)s Containing Naphthalene Units for Direct Methanol Fuel Cells (DMFCs). *Macromolecules* **2013**, *46* (9), 3452−3460.

(55) Lee, S. Y.; Kang, N. R.; Shin, D. W.; Lee, C. H.; Lee, K.-S. S.; Guiver, M. D.; Li, N.; Lee, Y. M. Morphological Transformation during Cross-Linking of a Highly Sulfonated Poly(Phenylene Sulfide Nitrile) Random Copolymer. *Energy Environ. Sci.* **2012**, *5* (12), 9795−9802.

(56) Calogirou, A.; Duane, M.; Kotzias, D.; Lahaniati, M.; Larsen, B. R. Polyphenylenesulfide, NOXON®, an Ozone Scavenger for the Analysis of Oxygenated Terpenes in Air. *Atmos. Environ.* **1997**, *31* (17), 2741−2751.

(57) Kutney, G. *Sulfur: History, Technology, Applications & Industry*, 2nd ed.; ChemTec PublishingToronto: Toronto, 2013.

(58) Worthington, M. J. H.; Kucera, R. L.; Chalker, J. M. Green Chemistry and Polymers Made from Sulfur. *Green Chem.* **2017**, *19* (12), 2748−2761.

(59) Chung, W. J.; Griebel, J. J.; Tae Kim, E.; Yoon, H.; Simmonds, A. G.; Jun Ji, H.; Dirlam, P. T.; Glass, R. S.; Jae Wie, J.; Nguyen, N. A.; Guralnick, B. W.; Park, J.; Somogyi, R.; Theato, P.; Mackay, M. E.; Sung, Y. C.; Kookheon, P. J. The Use of Elemental Sulfur as an Alternative Feedstock for Polymeric Materials. *Nat. Chem.* **2013**, *5*, 518−524.

(60) Ayala, V.; Maya, E. M.; García, J. M.; Campa, J. G. D. La; Lozano, A. E.; Abajo, J. De. Synthesis, Characterization, and Water Sorption Properties of New Aromatic Polyamides Containing Benzimidazole and Ethylene Oxide Moieties. *J. Polym. Sci., Part A: Polym. Chem.* **2005**, *43* (1), 112−121.

(61) Su, P.-H.; Lin, H.-L.; Lin, Y.-P.; Yu, T. L. Influence of Catalyst Layer Polybenzimidazole Molecular Weight on the Polybenzimidazole-Based Proton Exchange Membrane Fuel Cell Performance. *Int. J. Hydrogen Energy* **2013**, *38* (31), 13742−13753.

(62) Yao, Z.; Zhang, Z.; Wu, L.; Xu, T. Novel Sulfonated Polyimides Proton-Exchange Membranes via a Facile Polyacylation Approach of Imide Monomers. *J. Membr. Sci.* **2014**, *455*, 1−6.

(63) Zimmerman, D. A.; Koenig, J. L.; Ishida, H. Infrared Spectroscopic Analysis of Poly(p-Phenylene Sulfide). *Spectrochim. Acta, Part A* **1995**, *51* (13), 2397−2409.

(64) Gillham, J. K. Polymer Structure: Cross-Linking of a Polybenzimidazole. *Science* **1963**, *139* (3554), 494−495.

(65) Wang, S.; Zhang, G.; Han, M.; Li, H.; Zhang, Y.; Ni, J.; Ma, W.; Li, M.; Wang, J.; Liu, Z.; Zhnag, L.; Na, H. Novel Epoxy-Based Cross-Linked Polybenzimidazole for High Temperature Proton Exchange Membrane Fuel Cells. *Int. J. Hydrogen Energy* **2011**, *36* (14), 8412−8421.

(66) Seiffert, S. Scattering Perspectives on Nanostructural Inhomogeneity in Polymer Network Gels. *Prog. Polym. Sci.* **2017**, *66*, 1−21.

(67) Wisotzki, E. I.; Tempesti, P.; Fratini, E.; Mayr, S. G. Influence of High Energy Electron Irradiation on the Network Structure of Gelatin Hydrogels as Investigated by Small-Angle X-Ray Scattering (SAXS). *Phys. Chem. Chem. Phys.* **2017**, *19* (19), 12064−12074.

(68) Li, T.; Luo, F.; Fu, X.; Li, L.; Min, J.; Zhang, R.; Hu, S.; Zhao, F.; Li, X.; Zhang, Y.; et al. In Situ Synthesis of Star Copolymers Consisting of a Polyhedral Oligomeric Silsesquioxane Core and Poly(2,5-Benzimidazole) Arms for High-Temperature Proton Exchange Membrane Fuel Cells. *Int. J. Energy Res.* **2020**, 1−12.

(69) Vilčiauskas, L.; Tuckerman, M. E.; Melchior, J. P.; Bester, G.; Kreuer, K. D. First Principles Molecular Dynamics Study of Proton Dynamics and Transport in Phosphoric Acid/Imidazole (2:1) System. *Solid State Ionics* **2013**, *252*, 34−39.

(70) Lobato, J.; Cañizares, P.; Rodrigo, M. A.; Linares, J. J.; Aguilar, J. A. Improved Polybenzimidazole Films for H3PO4-Doped PBI-Based High Temperature PEMFC. *J. Membr. Sci.* **2007**, *306* (1−2), 47−55.

(71) Chang, Z.; Pu, H.; Wan, D.; Jin, M.; Pan, H. Effects of Adjacent Groups of Benzimidazole on Antioxidation of Polybenzimidazoles. *Polym. Degrad. Stab.* **2010**, *95* (12), 2648−2653.

(72) Chang, Z.; Pu, H.; Wan, D.; Liu, L.; Yuan, J.; Yang, Z. Chemical Oxidative Degradation of Polybenzimidazole in Simulated Environment of Fuel Cells. *Polym. Degrad. Stab.* **2009**, *94* (8), 1206−1212.